Magnetic domain structures and anisotropic in-plane transport in layered manganites

Y. Tokunaga, M. Tokunaga, and T. Tamegai
Department of Applied Physics, The University of Tokyo, 7-3-1 Hongo, Bunkyo-ku, Tokyo 113-8656, Japan
(Received 17 August 2004; published 19 January 2005)

The magnetic domain structures of layered manganites $(La_{1-z}R_z)_{1.2}Sr_{1.8}Mn_2O_7$ (R=Nd, z=0.4 and Pr, z=0.6) are studied by utilizing the magneto-optical imaging technique. Below transition fields from paramagnetic insulator to ferromagnetic metal, stripe like domains running perpendicular to the crystal-growth direction are observed. After applying sufficiently large fields for the transition, the domain structures become rather isotropic. Relation between domain structures and anisotropic in-plane transport properties is studied.

DOI: 10.1103/PhysRevB.71.012408 PACS number(s): 75.47.Lx, 64.60.Ak, 71.30.+h

In manganites, spin, charge, and orbital degrees of freedom couple inseparably, giving rise to many physically attractive phenomena, such as colossal magnetoresistance (CMR), charge ordering, orbital ordering, and phase separation (PS) into ferromagnetic metal (FMM) and antiferromagnetic insulator (AFI) phases.

In a double-layered perovskite manganite $La_{1.2}Sr_{1.8}Mn_2O_7$, $d_{x^2-y^2}$ obitals of Mn^{3+} are mainly occupied by e_g electrons. This orbital occupancy makes the ground state FMM with the *in-plane* easy axis.[1] By partially substituting smaller cations like Pr^{3+} or Nd^{3+} for La^{3+}, however, the ratio of lattice parameters, c/a, becomes larger. Such deformations of MnO_6 octahedra increase occupancy of $d_{3z^2-r^2}$ orbitals and suppress the FMM state because of a reduction of the transfer integral in the *ab* plane. Instead, the paramagnetic insulator (PI) state appears even at low temperatures. In PI states of $(La_{1-z}Nd_z)_{1.2}Sr_{1.8}Mn_2O_7$ (z=0.4) (LNSMO-0.4) and $(La_{1-z}Pr_z)_{1.2}Sr_{1.8}Mn_2O_7$ (z=0.6) (LPSMO-0.6), application of magnetic fields of tens of kOe induces FMM states with the *out-of-plane* easy axis.[2,3] This FMM state is metastable against the PI state, having a very long lifetime after removing the field at low temperatures. Memory effects of magnetoresistance, magnetization, magnetostriction, and magnetothermal conductivity are reported in Pr-substituted systems.[2,4–6]

For understanding the mechanism of the CMR phenomena, it will be helpful to investigate the microscopic magnetic domain structures in the CMR materials. Although there have been some reports about observations of magnetic domain structures in manganites in the solely ferromagnetic (FM) or the PS state between the antiferromagnetic (AFM) and the FM state by utilizing magneto-optical (MO) indicators,[7,8] magnetic force,[9,10] scanning superconducting quantum interference device (SQUID),[11] scanning Hall probe,[12] or Lorentz microscopes,[13] these studies are limited to the low-magnetic-field region. To study the CMR effect that occurs in large magnetic fields, observations of magnetic domains not only in the ground state but also in transient or metastable states are necessary. Here we present the first observations of structural changes of the magnetic domains before and after the magnetic field-induced PI-FMM transitions in LNSMO-0.4 and LPSMO-0.6 up to H=5 kOe with using an MO imaging.

The MO imaging is the technique that visualizes magnetic field distributions near the sample surface by utilizing the Faraday effect of an MO indicator film mounted on the sample.[14] As an MO indicator film, we utilize a paramagnetic EuSe thin film deposited on a cover glass, which has been historically used for studying magnetic flux behavior in type-II superconductors.[15] Although the useful temperature range of the EuSe film is limited below about 20 K, the useful magnetic field range is relatively wide (<30 kOe). We use a polarizing microscope with a long lens barrel, which can be inserted into a superconducting magnet installed in a He cryostat. We can apply magnetic fields up to 90 kOe perpendicular to the observation plane. The spatial resolution, mainly limited by the gap between the sample and the indicator film, is a few μm. Single crystals of LNSMO-0.4 and LPSMO-0.6 are grown in an infrared image furnace by the floating-zone (FZ) method. Cleaved flat surfaces (*ab* plane) are used for MO measurements. First we apply H_{max}, then decrease H to H_{pic}, and obtain images. All images are taken at 10 K. Electrical transport properties are measured by using the conventional four-probe method. Electrical pads are formed by heat-treatment-type silver paste. The sample dimensions used in the transport measurements are typically $2000\times400\times50$ μm^3.

Figure 1 shows isothermal magnetization curves of LNSMO-0.4 at 10 K measured by using a SQUID magnetometer (Quantum Design MPMS). To check the presence of the memory effect, we measured M-H half-loops successively, changing the maximum field (H_{max}) up to 40 kOe.

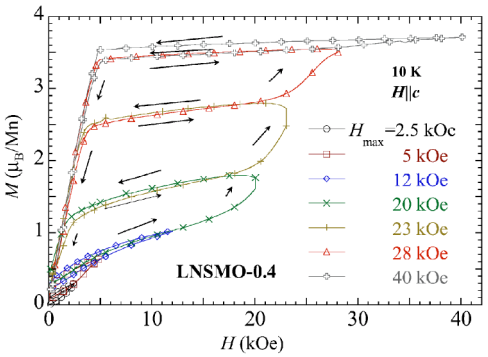

FIG. 1. (Color online) Magnetic field dependence of bulk magnetization of LNSMO-0.4 at 10 K. Successive minor M-H loops taken between H=0 and H_{max} by gradually increasing H_{max} up to 40 kOe are superimposed.

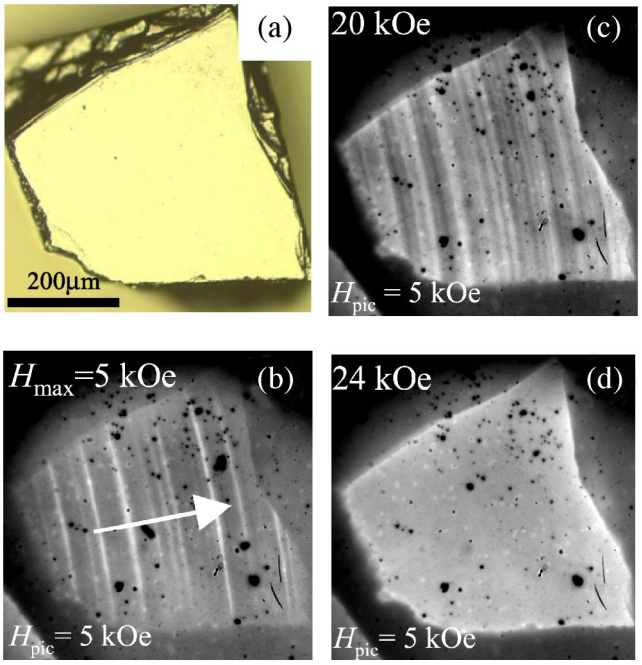

FIG. 2. (Color online) (a) A polarizing microscope image of the cleaved *ab* plane of LNSMO-0.4. MO images of the cleaved surface taken at H_{pic}=5 kOe and 10 K for H_{max}'s (b) 5 kOe, (c) 20 kOe, and (d) 24 kOe. The white arrow in (b) indicates the crystal-growth direction by the FZ method. Black spots in MO images are not magnetic signals but accidental attachments on the lens or scratches on the MO indicator film.

Each curve in the field-decreasing process from H_{max} coincides with that in the successive field-increasing process from zero field. In other words, the sample remembers the state at H_{max} even after the field is removed. Thus we can obtain information of local magnetization at H_{max}, even if we observe the domain structure after reducing the field from H_{max}. As can be seen from Fig. 1, the volume fraction of the ferromagnetic domains increase as H_{max} is increased. Since the reorientation of ferromagnetic domains occur below 5 kOe, we visualize the evolution of the PI-FMM transition by taking MO images at H_{pic}=5 kOe after applying various H_{max}.

Figure 2(a) shows a polarizing microscope image of a cleaved surface of LNSMO-0.4 taken at room temperature. The surface looks flat and homogeneous. Figures 2(b)–2(d) show MO images at H_{pic}=5 kOe after applying H_{max}=5–24 kOe, which are smaller than the field to complete the PI-FMM transition (see Fig. 1). Bright and dark contrasts reflect the variation of the magnetic induction perpendicular to the *ab* plane. Black spots on the sample are not magnetic signals but accidental attachments on the lens or scratches on the MO indicator film. We observe stripelike magnetic structures running across the sample. These structures are not related to the surface topology of the sample, as seen in Fig. 2(a). Bright stripes always run perpendicular to the crystal-growth direction indicated by the white arrow in Fig. 2(b). The bright stripes in the image gradually increase their widths and number as H_{max} is increased, before the entire sample finally becomes magnetically saturated above H_{max}=24 kOe, as shown in Fig. 2(d).

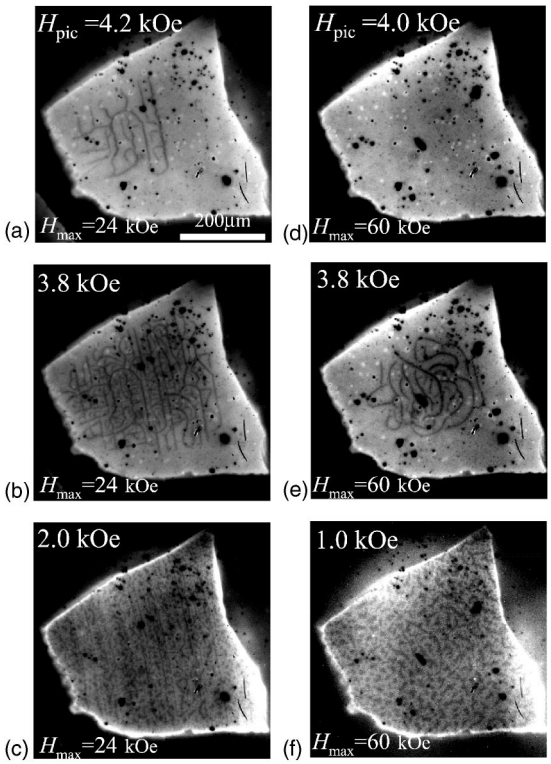

FIG. 3. Nucleation and formation process of magnetic domains with decreasing magnetic fields after applying H_{max} at 10 K. Images (a)–(c) are at (a) 4.2 kOe, (b) 3.8 kOe, and (c) 2.0 kOe with H_{max}=24 kOe, while images (d)–(f) are taken at (d) 4.0 kOe, (e) 3.8 kOe, and (f) 1.0 kOe with H_{max}=60 kOe.

Figure 3 shows the images of nucleation and formation of magnetic domain patterns in the magnetic-field-decreasing process after applying H_{max} at 10 K. Reduction of H_{pic} to less than 5 kOe causes nucleation of magnetic domains in the ferromagnetic region. Figures 3(a)–3(c) show MO images taken in the field-decreasing process from H_{max}=24 kOe. Stripe magnetic domains show up as H_{pic} is decreased. It should be noted that the magnetic domains show some correlation with bright stripes seen in Figs. 2(b) and 2(c). Although the MO image in Fig. 2(d) shows almost homogeneous magnetization at H_{max}=24 kOe, the stripe structures perpendicular to the growth direction remain in the sample. On the contrary, application of larger fields removes this correlation completely. Figures 3(d)–3(f) are MO images in the field-decreasing process from H_{max}=60 kOe. In these images, formed magnetic domains become isotropic and show no correlation with stripe structures observed in Figs. 2(b) and 2(c).

We perform similar experiments on LPSMO-0.6 and observe similar stripelike structures. We prepared two rods of crystals with different growth rates 10 and 5 mm/h. Figures 4(a) and 4(b) are MO images on the cleaved *ab* plane of LPSMO-0.6 taken at T=10 K and H_{pic}=2 kOe after application of H_{max}=35 kOe. For LPSMO-0.6, this H_{max} is smaller than the saturation field at 10 K. The spacing of stripes in Fig. 4(a) is larger than that in Fig. 4(b), indicating that those spacings depend on the crystal-growth rate. Thus we believe that these stripe structures originate from the striation with

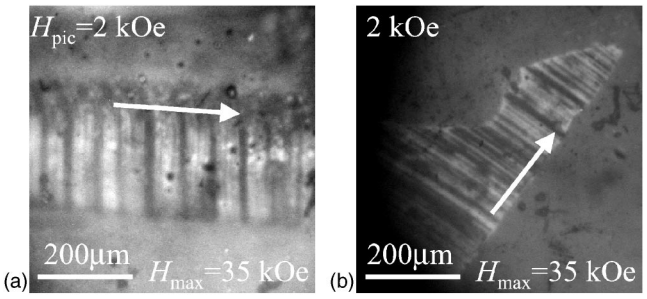

FIG. 4. MO images of magnetic stripe structures in the *ab* plane of LPSMO-0.6 crystals grown at (a) 10 mm/h and (b) 5 mm/h taken under H_{pic}=2 kOe after applying H_{max}=35 kOe at 10 K. White arrows indicate the crystal-growth direction by the FZ method.

either modulation of chemical compositions or lattice parameters frozen in the process of crystal growth.[16] In both cases of LNSMO-0.4 and LPSMO-0.6, remanent ferromagnetic structures observed at 10 K are stable and show no topological changes at least 1 day after removing the field. This result reflects the long relaxation time of the system.[2,6]

To clarify how these stripe structures affect the transport properties, we measured in-plane resistivity (ρ) parallel and perpendicular to the crystal-growth direction. A plate cleaved from the grown rod of LNSMO-0.4 is first polished to a thickness of about 50 μm. Two adjacent rectangular pieces are cut from this thin plate for the resistivity measurements, with its long axis parallel and perpendicular to the crystal-growth direction for the resistivity measurement along each direction. We confirmed the presence of magnetic stripelike structures in these pieces (not shown).

The inset of Fig. 5(a) shows the *M*-*H* curves of the two samples for resistivity measurements. *M*-*H* curves for both samples are almost indistinguishable. The inset of Fig. 5(b) shows the magnetic field dependence of resistivity parallel and perpendicular to the magnetic stripes observed in the MO measurements at 10 K. As expected, resistivity perpendicular to the stripes ($\rho_\perp$) is tens of times larger than that parallel to the stripes ($\rho_\parallel$) at low magnetic fields before the PI-FMM transition ($\rho_\perp/\rho_\parallel$=46 at H=0). After applying sufficiently large magnetic fields for the PI-FMM transition, this anisotropic behavior is strongly suppressed. Figures 5(a) and 5(b) show the temperature dependence of $\rho_\perp$ and $\rho_\parallel$, taken at several values of magnetic fields between 0 and 50 kOe in field-cooling conditions. In the zero-magnetic-field condition, the resistivity is insulative along both directions down to the lowest temperature. This temperature dependence is different from that reported by Moritomo *et al.*,[3] probably because of a slight difference in chemical compositions. The temperature dependence of the resistivity in our samples is rather similar to that reported for LPSMO-0.6, which is insulating in all temperature range under zero magnetic field and shows huge magnetoresistance (magnetoresistance ratio $\sim 10^6$ at 10 K).[17] The residual resistivity of our sample along each direction is $\sim$1 mΩ cm at 50 kOe, which is lower than values in Refs. 2–4. Judging from this fact, our crystals are of better quality. At high temperatures or high magnetic fields, the resistivity is almost isotropic along two directions.

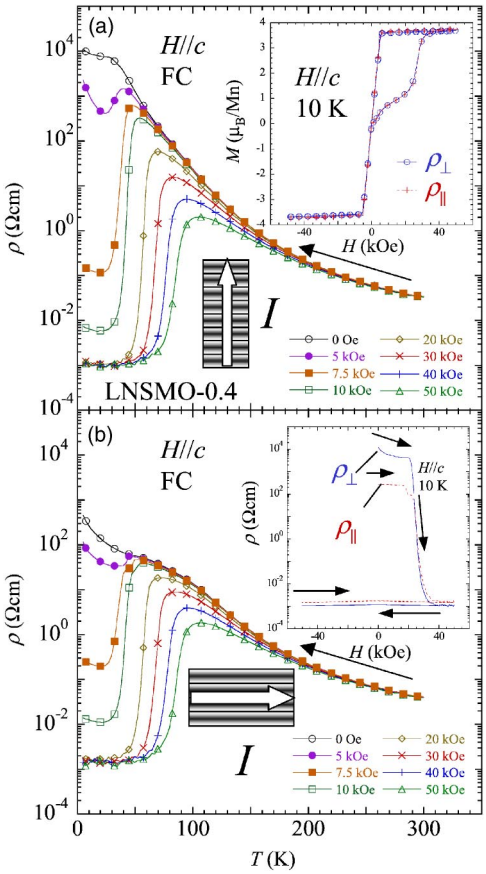

FIG. 5. (Color online) Temperature dependence of resistivity (a) perpendicular and (b) parallel to the magnetic stripes, taken under several values of magnetic fields between 0 and 50 kOe in field-cooling conditions. The inset of (a) shows *M*-*H* curves of the two samples for resistivity measurements taken at 10 K. Two curves are superimposed. The inset of (b) shows magnetic field dependence of resistivity parallel and perpendicular to the magnetic stripes at 10 K.

However, at low magnetic fields and low temperatures, $\rho_\perp$ becomes more than 10 times larger than $\rho_\parallel$.

As can be seen in Fig. 1 and Fig. 3(d), 5 kOe is large enough to align the magnetic moment along the magnetic field direction in the FMM domain at 10 K. Although the sample shows anisotropic electrical conduction at low fields, the difference between $\rho_\perp$ and $\rho_\parallel$ is smaller than that expected in the situation where FMM stripes (metallic paths) run across the sample. In the present MO observations, magnetic structures smaller than the experimental resolution of a few microns are averaged out. So we believe that each observed bright stripe is not a single FMM domain, but it is a region where the volume fraction of small FMM clusters is large. Therefore, metallic paths are not necessarily connected along the bright stripes. Expansion of these stripes means either increase of the number or the size of ferromagnetic clusters. The fact that anisotropic resistivity is observed even at zero magnetic field means that ferromagnetic domains exist even at zero magnetic field with spatially anisotropic distribution. In the metastable FMM state, the entire sample is magnetically isotropic in the *ab* plane, as can be seen in the

magnetic domain structures in Figs. 3(d)–3(f). The corresponding resistivity also becomes rather isotropic.

Although the scale is different, the observed magnetic structural changes are analogous to $Pr_{1-x}Ca_xMnO_3$ ($x=0.33$), showing similar magnetic-field-induced AFI-FMM transitions at low temperatures.[18] In this material, the magnetic field dependence of electrical phase separation is studied by small-angle neutron scattering experiments.[19,20] The presence of two types of domains, ferromagnetic and antiferromagnetic sheets with thicknesses of about 2.5 nm, forming "red cabbage" in the ground state is reported.[19,20] By applying magnetic fields, ferromagnetic sheets gradually increase their thickness, until the system becomes a homogeneous ferromagnet. When the magnetic field is decreased, the system remains entirely ferromagnetic, forming Weiss domains at low magnetic fields. In this case, however, the distributions of FM and AFM sheets are isotropic, leading to isotropic electrical conduction.

The presence of observed stripe structures indicates the existence of some kinds of modulation along the crystal-growth direction. In the metastable FMM state, this modulation simply vanishes or does not have much effect on magnetic domain structures and transport properties even if it exists. From the fact that similar stripe structures are also observed in LPSMO-0.6 samples (see Fig. 4), we believe that this modulation is intrinsic to these systems. In these systems, the phase diagram changes drastically depending not only on the hole-doping level, but also on the c/a ratio.[3] Small modulations of lattice parameters or chemical compositions may change the robustness of $d_{3z^2-r^2}$ orbital against external magnetic fields and cause the modulation of the PI-FMM transition fields along the crystal-growth direction by the FZ method. To investigate the origin of the magnetic stripe structure and anisotropic electrical transport, we performed EPMA-EDS scans parallel and perpendicular to the observed magnetic stripe structures. The fluctuation of the compositional ratio thus determined is within the error bar (about 1 %) and shows no correlation with the crystal growth direction. So the anisotropy may originate from the modulation of oxygen deficiencies or crystallographic defects along the crystal growth direction. A slight residual strain introduced during the crystal growth can also cause the variation of transition fields.[21] Further experiments are needed to clarify the origin of the magnetic stripe structures running perpendicular to the crystal-growth direction.

In conclusion, we have observed magnetic domain structures of $(La_{1-z}R_z)_{1.2}Sr_{1.8}Mn_2O_7$ ($R=$Nd, $z=0.4$ and Pr, $z=0.6$) before and after the magnetic-field-induced transition from paramagnetic insulator to ferromagnetic metal by magneto-optical imaging. Stripelike structures running perpendicular to the crystal-growth direction are observed before PI-FMM transition, which transformed into rather isotropic domain structures after FMM transition. In-plane transport properties show a good correlation with the magnetic domain structures.

The authors thank F. Sakai for help in EPMA-EDS measurements. This work is supported by a Grant-in-Aid for Scientific Research from the Ministry of Education, Culture, Sports, Science and Technology.

[1] Y. Moritomo, A. Asamitsu, H. Kuwahara, and Y. Tokura, Nature (London) **380**, 141 (1996).
[2] I. Gordon, P. Wagner, V. V. Moshchalkov, Y. Bruynseraede, M. Apostu, R. Suryanarayanan, and A. Revcolevschi, Phys. Rev. B **64**, 092408 (2001).
[3] Y. Moritomo, Y. Maruyama, T. Akimoto, and A. Nakamura, Phys. Rev. B **56**, R7057 (1997).
[4] M. Apostu, R. Suryanarayanan, A. Revcolevschi, H. Ogasawara, M. Matsukawa, M. Yoshizawa, and N. Kobayashi, Phys. Rev. B **64**, 012407 (2001).
[5] M. Matsukawa, M. Narita, T. Nishimura, M. Yoshizawa, M. Apostu, R. Suryanarayanan, A. Revcolevschi, K. Itoh, and N. Kobayashi, Phys. Rev. B **67**, 104433 (2003).
[6] M. Matsukawa, M. Chiba, K. Akasaka, R. Suryanarayanan, M. Apostu, A. Revcolevschi, S. Nimori, and N. Kobayashi, Phys. Rev. B **70**, 132402 (2004).
[7] U. Welp, A. Berger, D. J. Miller, V. K. Vlasko-Vlasov, K. E. Gray, and J. F. Mitchell, Phys. Rev. Lett. **83**, 4180 (1999).
[8] U. Welp, A. Berger, V. K. Vlasko-Vlasov, Q. A. Li, K. E. Gray, and J. F. Mitchell, Phys. Rev. B **62**, 8615 (2000).
[9] R. Desfeux, S. Bailleul, A. Da Costa, W. Prellier, and A. M. Haghiri-Gosnet, Appl. Phys. Lett. **78**, 3681 (2001).
[10] H. Oshima, Y. Ishihara, M. Nakamura, and K. Miyano, Phys. Rev. B **63**, 094420 (2001).
[11] Y. Okimoto, Y. Ogimoto, M. Matsubara, Y. Tomioka, T. Kageyama, T. Hasegawa, H. Koinuma, M. Kawasaki, and Y. Tokura, Appl. Phys. Lett. **80**, 1031 (2002).
[12] T. Fukumura, H. Sugawara, T. Hasegawa, K. Tanaka, H. Sakaki, T. Kimura, and Y. Tokura, Science **284**, 1969 (1999).
[13] S. Mori, R. Shoji, N. Yamamoto, T. Asaka, Y. Matsui, A. Machida, Y. Moritomo, and T. Katsufuji, Phys. Rev. B **67**, 012403 (2003).
[14] Ch. Jooss, J. Albrecht, H. Kuhn, S. Leonhardt, and H. Kronmüller, Rep. Prog. Phys. **65**, 651 (2002).
[15] Th. Schuster, M. R. Koblischka, B. Ludescher, N. Moser, and H. Kronmüller, Cryogenics **31**, 811 (1991).
[16] M. Yasugaki, M. Tokunaga, N. Kameda, and T. Tamegai, Phys. Rev. B **67**, 104504 (2003).
[17] P. Wagner, I. Gordon, V. V. Moshchalkov, Y. Bruynseraede, M. Apostu, R. Suryanarayanan, and A. Revcolevschi, Europhys. Lett. **58**, 285 (2002).
[18] H. Yoshizawa, H. Kawano, Y. Tomioka, and Y. Tokura, Phys. Rev. B **52**, R13 145 (1995).
[19] S. Mercone, V. Hardy, C. Martin, C. Simon, D. Saurel, and A. Brulet, Phys. Rev. B **68**, 094422 (2003).
[20] C. Simon, S. Mercone, N. Guiblin, C. Martin, A. Brulet, and G. Andre, Phys. Rev. Lett. **89**, 207202 (2002).
[21] Y. Tokura and N. Nagaosa, Science **288**, 462 (2000).